Front. Chem. Sci. Eng. 2022, 16(1): 81–91
https://doi.org/10.1007/s11705-021-2049-7

RESEARCH ARTICLE

Crown ether-thiourea conjugates as ion transporters

Zhixing Zhao[1], Bailing Tang[1], Xiaosheng Yan (✉)[1], Xin Wu (✉)[2], Zhao Li[1], Philip A. Gale (✉)[2,3], Yun-Bao Jiang (✉)[1]

1 Department of Chemistry, College of Chemistry and Chemical Engineering, The MOE Key Laboratory of Spectrochemical Analysis and Instrumentation, iChEM, Xiamen University, Xiamen 361005, China
2 School of Chemistry (F11), The University of Sydney, Sydney, NSW 2006, Australia
3 The University of Sydney Nano Institute (Sydney Nano), The University of Sydney, Sydney, NSW 2006, Australia

Abstract Na^+, Cl^- and K^+ are the most abundant electrolytes present in biological fluids that are essential to the regulation of pH homeostasis, membrane potential and cell volume in living organisms. Herein, we report synthetic crown ether-thiourea conjugates as a cation/anion symporter, which can transport both Na^+ and Cl^- across lipid bilayers with relatively high transport activity. Surprisingly, the ion transport activities were diminished when high concentrations of K^+ ions were present outside the vesicles. This unusual behavior resulted from the strong affinity of the transporters for K^+ ions, which led to predominant partitioning of the transporters as the K^+ complexes in the aqueous phase preventing the transporter incorporation into the membrane. Synthetic membrane transporters with Na^+, Cl^- and K^+ transport capabilities may have potential biological and medicinal applications.

Keywords ion transport, thiourea, crown ether, symport

1 Introduction

A wide range of synthetic ion transporters have been developed during the past decades owing to their potential biomedical applications [1,2] in treating cancer and channelopathies like cystic fibrosis [3,4], Bartter syndrome [5] and Dent's disease [6]. Anions transporters were designed to transport HCO_3^-, F^-, Cl^-, I^- and SO_4^{2-} [7–11], among which Cl^- is the most commonly targeted anion. Besides cystic fibrosis, dysregulation of Cl^- transport will also indirectly result in exocrine pancreatic failure, intestinal blockage and male infertility [12]. Hence, synthetic Cl^- transporters have been developed, either working as channels [13] or carriers [14]. Transmembrane cation transport also plays key roles in cellular processes. The concentrations of Na^+ and K^+ in cells are regulated with the concentration gradient generated by Na^+/K^+ ATPase. The concentration of Na^+ is ~10 $mmol \cdot L^{-1}$ inside and ~150 $mmol \cdot L^{-1}$ outside, however, for K^+, the extracellular concentrations (5 $mmol \cdot L^{-1}$) are lower than those in the cytoplasm (150 $mmol \cdot L^{-1}$) [15]. In biological systems, Na^+ and K^+ channels work synergistically in processes such as initiating and regulating action potentials in neurons and cells [16,17]. Mutations of Na^+ channels are found to be closely linked to inherited epilepsy, migraine, periodic paralysis and chronic pain syndromes [18,19]. In addition, cardiac arrhythmias, deafness and epilepsy involved mutations of several critical K^+ channels [20,21].

Due to the indispensable role of Na^+, K^+ and Cl^- in nearly every animal cell type [22,23], synthetic transporters for Na^+, K^+ and Cl^- have attracted significant attention. In addition to cation transporters and anion transporters, several researcher groups have developed ion-pair symporters [24–27], which contain at least one cation binding site and one anion binding site. Calix[4]pyrrole was reported by Gale and co-workers to transport CsCl as an ion-pair complex [24,25]. Smith and co-workers reported transporters containing an amide and an azacrown ether moieties to achieve the co-transport of NaCl or KCl [26]. Azacrown ethers were also combined with a urea or a squaramide motif to selectively transport KCl [27,28]. However, due to the high hydration energy of Na^+ [29,30] and the higher affinity of 15-crown-5 and 18-crown-6 for K^+ under certain conditions [29], the selective transport of Na^+ over K^+ is challenging.

Herein, we synthesized bilateral crown ether-thiourea conjugates **Azo-2C5** and **Azo-2C6** as ion transporters (Scheme 1), which were designed based on the following considerations: (i) crown ethers, benzo-15-crown-5 in

Received December 15, 2020; accepted February 14, 2021

E-mails: xshyan@xmu.edu.cn (Yan X), xin.wu@sydney.edu.au (Wu X), philip.gale@sydney.edu.au (Gale PA), ybjiang@xmu.edu.cn (Jiang Y)

Azo-2C5 and benzo-18-crown-6 in **Azo-2C6**, are employed to bind and transport Na^+ and K^+ across membrane [27,31,32] and (ii) *N*-amidothiourea groups, which exhibit enhanced anion binding ability in comparison to conventional *N*-alkyl and *N*-arylthiourea counterparts, by virtue of an anion-induced conformation change in the N–N single bond and a multivalent hydrogen-bonding network [33,34]. Thus *N*-amidothiourea moieties are employed for Cl^- binding and transmembrane transport. (iii) An azobenzene group is utilized as linker to improve the lipophilicity of the transporters [35,36], facilitating ion transmembrane transport. Control compounds **Ph-2C5** and **Azo-C5** (Scheme 1) were designed to investigate the significance of azobenzene motif and bilateral structure for ion transport, respectively. We found that **Azo-2C5** could transport Na^+ and Cl^- across the membrane with high activity, while **Azo-2C6** exhibited a higher Cl^- transport activity and a much lower Na^+ transport activity owing to the mismatch of Na^+ with 18-crown-6 [37]. Surprisingly, neither transporter showed K^+ transport activity, and the presence of K^+ at high concentrations substantially hindered the transport of Na^+ and Cl^-. This unique phenomenon has been shown by ultra-violet-visible spectroscopy (UV-Vis) studies to originate from the predominant partitioning of the transporters in the aqueous phase when K^+ was present in high concentrations.

2 Experimental

2.1 Materials

4,4'-Diaminoazobenzene, 1,1'-thiocarbonyldiimidazole, methyl 3,4-dihydroxybenzoate, bis[2-(2-chloroethoxy) ethyl]ether, pentaethylene glycol dichloride 1,4-phenylene diisothiocyanate and 4-phenylazophenyl isothiocyanate were purchased from J&K Scientific Ltd. 1-Palmitoyl-2-oleoylphosphatidylcholine (POPC) and dipalmitoylphosphatidylcholine (DPPC) were purchased from Avanti Polar Lipids. Triton X-100, valinomycin (Vln), carbonyl cyanide 4-(trifluoromethoxy)phenylhydrazone (FCCP), calcein, 8-hydroxypyrene-1,3,6-trisulfonic acid trisodium salt (HPTS), 6-methoxy-*N*-(3-sulfopropyl)quinolinium (SPQ), sodium gluconate (NaGlc), potassium gluconate, *N*-methyl-D-glucamine chloride (NMDG-Cl), 4-(2-hydroxyerhyl)piperazine-1-erhanesulfonic acid (HEPES) were purchased from Sigma Aldrich Co. and used directly without purification. Dimethyl sulfoxide-D_6 was purchased from Cambridge Isotope Laboratories Inc. All

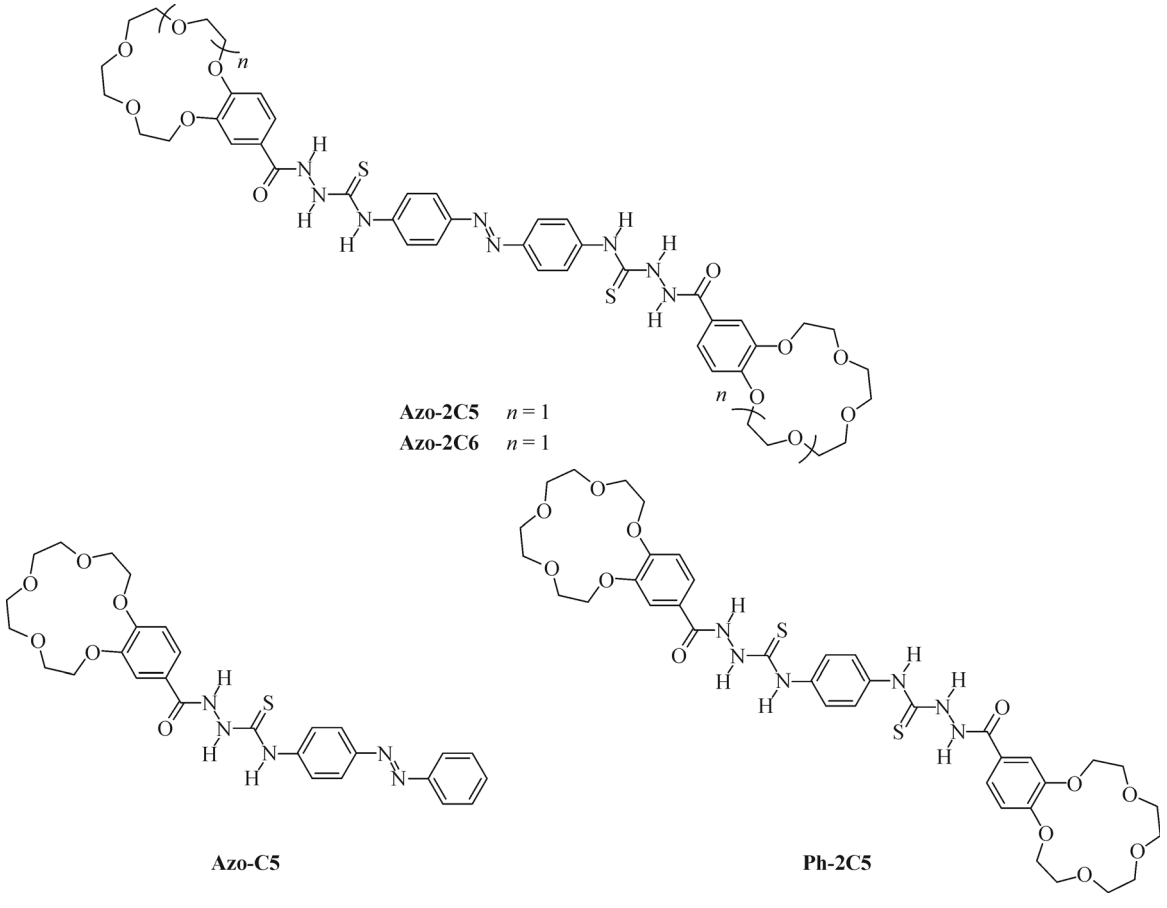

Scheme 1 Molecule structures of synthetic transporters **Azo-2C5**, **Azo-2C6**, and control compounds **Azo-C5**, **Ph-2C5**.

other starting materials were obtained from Sinopharm Chemical Reagent Ltd.

2.2 Instrumentation

^{1}H and ^{13}C nuclear magnetic resonance (NMR) spectra were recorded on Bruker AV500MHz, AV600MHz or AV850MHz spectrometers. High-resolution mass spectra were acquired on a Bruker micro TOF-Q-II mass spectrometer. Absorption spectra were recorded on Shimadzu UV-2700 UV-Vis spectrophotometer. Fluorescence spectra were obtained on a Horiba Fluorolog-3 spectrometer.

2.3 Ion transport study and the EC_{50} measurement

2.3.1 Preparation of large unilamellar vesicles (LUVs)

LUVs (mean diameter 200 nm) of POPC loaded with pH-sensitive fluorescence dye HPTS (0.1 mmol·L^{-1}) were prepared by freeze/thaw cycles. A chloroform solution (50 mL) of POPC (10 mg) was slowly evaporated by using a rotary evaporator and dried under high vacuum at room temperature for 4 h. The obtained lipid film was rehydrated by mixing with 1 mL salt solution (100 mmol·L^{-1} NaGlc, 10 mmol·L^{-1} HEPES, 0.1 mmol·L^{-1} HPTS, pH 7.0) and vortexing for 2 min. The mixtures were subjected to 10 freeze-thaw cycles and extruded through a 0.22 μm polycarbonate membrane at least 5 times. To separate the un-entrapped HPTS, the lipid suspension (0.76 mL, 10 mmol) was transferred to a size exclusion chromatography (stationary phase: Sephadex G-50; mobile phase: 100 mmol·L^{-1} NaGlc, 10 mmol·L^{-1} HEPES, pH 7.0) and eluted with the mobile phase to acquire a 5 mL lipid stock solution containing 2 mmol·L^{-1} of lipid.

2.3.2 Na^+ transport study

In the Na^+ transport study, 0.1 mL of the lipid stock solution was added to 1.88 mL buffer solution (100 mmol·L^{-1} NaGlc, 10 mmol·L^{-1} HEPES, pH 8.0) to generate a pH gradient. DMSO solution (20 μL) with or without transporters was added at time 0. The pH changing inside the LUVs was monitored by fluorescence of HPTS (λ_{ex} = 454 nm, λ_{em} = 510 nm). At 300 s, 20% Triton X-100 (10 μL) was added as detergent to lysate the LUVs for calibration. The fractional fluorescence intensity (I_f) was calculated based on Eq. (1):

$$I_f = \frac{R_t - R_0}{R_f - R_0} \times 100\%, \quad (1)$$

where R_t is the fluorescence intensity at time t, R_f is the final fluorescence intensity obtained by the addition of detergent, R_0 is the fluorescence intensity at the start time. Different concentrations of transporter molecules were added to obtain a series of fractional fluorescence intensity (I_f). Fitting I_f *vs*. molecule concentration according to Eq. (2):

$$y = y_0 + (y_{max} - y_0)\frac{x^n}{K + x^n}, \quad (2)$$

where y is the value of I_f corresponding to the carrier molecule loaded at concentration x, y_0 is the I_f value measured when compound has not been added, y_{max} is maximum I_f value, n is the Hill coefficient, K is the EC_{50} value. In this work, the concentration of LUVs is fixed at 100 μmol·L^{-1}.

The methodologies for tests of other transport activities are similar, which are described in detail in the Electronic Supplementary Material (ESM).

3 Results and discussions

3.1 Transport activities of Na^+ and Cl^-

The ion transport activities of **Azo-2C5** were tested in POPC based LUVs (mean diameter 200 nm) with encapsulated pH-sensitive fluorescence dye HPTS (Figs. 1 and 2). As the transporter contains both anion and cation recognition motifs, i.e., *N*-amidothiourea and crown ether moieties, the transport processes are studied by two separate experiments. In a Na^+ transport assay, NaGlc (100 mmol·L^{-1}) was used (Fig. 1(a)) based on the consideration that gluconate is too hydrophilic to pass through the hydrophobic membrane even with an anion transporter [38]. In a Cl^- transport assay (Fig. 2(a)), NMDG-Cl solution (100 mmol·L^{-1}) was used as the inert $NMDG^+$ rules out the possibility of cation transport [38]. The transport rate increased rapidly with increasing the concentrations of the transporter and the fluorescence response of HPTS reached a platform of 68% for Na^+ (Figs. 1(b) and 1(c)) and 62% for Cl^- (Figs. 2(b) and 2(c)). The plots can be fitted well utilizing the Hill equation and the corresponding parameters to give half maximal effective concentrations (EC_{50}) and Hill coefficients (n) values. The EC_{50} values for Na^+ (0.12 μmol·L^{-1}) and Cl^- (0.12 μmol·L^{-1}) are nearly the same, and the Hill coefficients for both transport processes are slightly higher than 1. The Hill coefficients indicate that the transporter is more likely to function as a monomer during Na^+ and Cl^- transport processes [39]. When NaCl was used as the internal and external salt (Fig. S1(a), cf. ESM), a similar EC_{50} of 0.15 μmol·L^{-1} and a similar Hill coefficient close to 1 were determined (Fig. S1(c)), thus a 1:1:1 (**Azo-2C5**:Na^+:Cl^-) stoichiometry could be expected for the symport of Na^+ and Cl^- (see below). No change in the transport rate of Na^+ and Cl^- was observed with the addition of a H^+ ionophore FCCP (Figs. S(2) and S3(b), cf. ESM), indicating that H^+ transport by **Azo-2C5** is likely not the rate-limiting process. A limited maximum activity of 70%

was observed (Fig. 1), and we assumed that the aggregation of the transporters in solution could be responsible, which limited the delivery of the transporters to the vesicles [40].

Compared with **Azo-2C5**, **Azo-2C6** has a significantly reduced transport activity for Na^+ (Fig. 1, 0.12 μmol·L^{-1} for EC_{50} of **Azo-2C5**; EC_{50} of **Azo-2C6** is not detectable), but a better transport activity for Cl^- (Fig. 2, 0.12 μmol·L^{-1} for EC_{50} of **Azo-2C5**; 0.05 μmol·L^{-1} for EC_{50} of **Azo-2C6**). The former is likely due to the mismatch between the cavity size of 18-crown-6 in **Azo-2C6** (134–143 pm) and the size of Na^+ (95 pm) [37]. The latter is ascribed to the higher binding affinity of **Azo-2C6** with Cl^- than those of **Azo-2C5** (Figs. S4 and S5, cf. ESM. For **Azo-2C6** in acetonitrile, K_{11} = 1915 L·mol^{-1}, K_{12} = 424 L·mol^{-1}; for **Azo-2C5** in acetonitrile, K_{11} = 1250 L·mol^{-1}, K_{12} = 341 L·mol^{-1}). An experiment employing FCCP (Fig. S3(c)) also indicated that H^+ transport by **Azo-2C6** is likely not the rate-limiting process. The reference compounds, **Ph-2C5** and **Azo-C5** display nearly no transport activity no matter what salt solution was used (Figs. S6–S8, cf. ESM). The inactivity of **Ph-2C5** indicates the essential role of azobenzene scaffold in facilitating the ion transport, which is ascribed to the lower lipophilicity of benzene than azobenzene motif. Notably, unilateral compound **Azo-C5** resembles a classic surfactant structure containing a polar head-group and a lipophilic tail, which is known to be detrimental to the transmembrane transport [41], underscoring the importance of bilateral structure of **Azo-2C5** in ion transport.

To obtain direct evidence for Na^+ and Cl^- transport, ^{23}Na NMR and SPQ experiments were conducted respectively. In the NMR experiment (Fig. S9, cf. ESM), $DyCl_3$ was added to discriminate the signals from intra- and extravesicular solutions by upfield shifting of outer ^{23}Na peak [32]. The NMR spectra at different incubation time confirmed the Na^+ transport ability of **Azo-2C5**. In the SPQ experiment (Fig. 3), as the inert NMDG can not pass through the membrane, the SPQ experiment showed relatively slower influx of Cl^- when the outer salt solution was NMDG-Cl (Figs. 3(a) and 3b). Replacing the NMDG-Cl with NaCl provides the transportable cation and hence the fluorescence quenching was observed (Figs. 3(c) and 3 (d)), suggesting the symport of Na^+/Cl^-. SPQ experiments, together with the ^{23}Na NMR experiment, confirmed that **Azo-2C5** can act as a symporter for NaCl.

3.2 Influence of K^+ on the transport activities

18-Crown-6 moiety has a cavity radius of 134–143 pm,

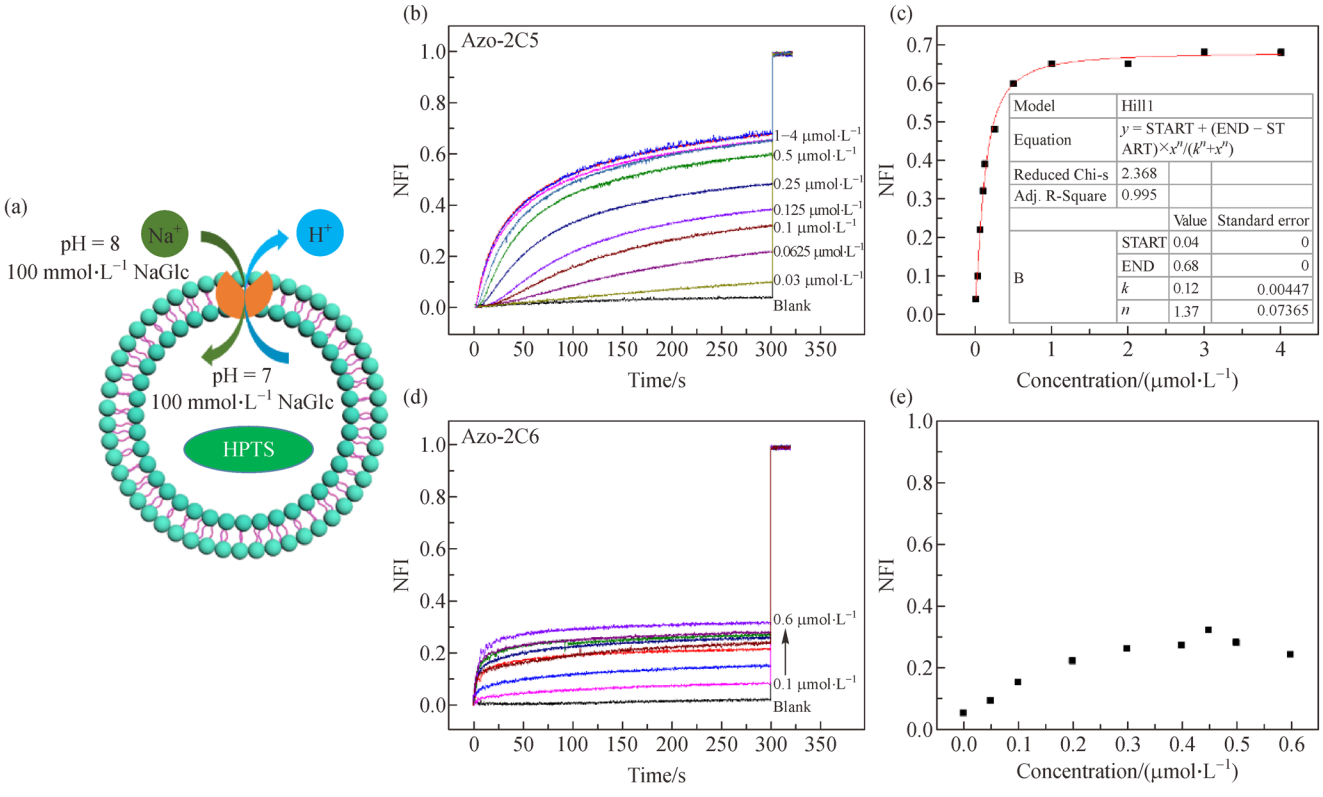

Fig. 1 (a) Schematic representation of quantitative measurement of Na^+ transport conducted by using a pH gradient of 7 inside and 8 outside in LUVs (mean diameter 200 nm) encapsulating pH-sensitive dye HPTS. Inside LUVs: 0.1 mmol·L^{-1} HPTS, 100 mmol·L^{-1} NaGlc, 10 mmol·L^{-1} HEPES, pH 7.0. Outside LUVs: 100 mmol·L^{-1} NaGlc, 10 mmol·L^{-1} HEPES, pH 8.0. Normalized fluorescence intensity (NFI) obtained by addition of different concentrations of **Azo-2C5** ((b) 0–4 μmol·L^{-1}) and **Azo-2C6** ((d and e) 0–0.6 μmol·L^{-1}). (c) Hill analysis of Na^+ transport facilitated by **Azo-2C5**.

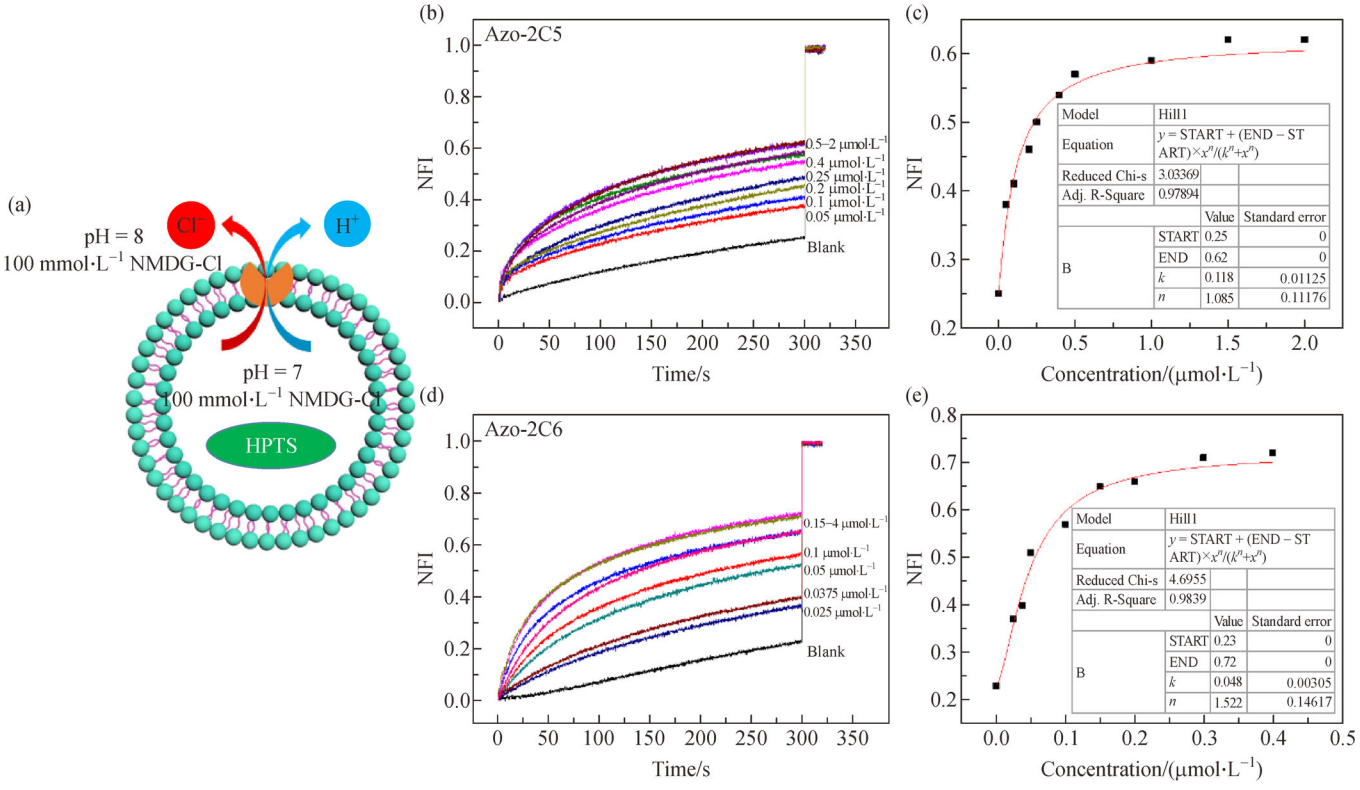

Fig. 2 (a) Schematic representation of quantitative measurement of Cl^- transport conducted by using a pH gradient of 7 inside and 8 outside in LUVs (mean diameter 200 nm) encapsulating pH-sensitive dye HPTS. Inside LUVs: 0.1 mmol·L^{-1} HPTS, 100 mmol·L^{-1} NMDG-Cl, 10 mmol·L^{-1} HEPES, pH 7.0. Outside LUVs: 100 mmol·L^{-1} NMDG-Cl, 10 mmol·L^{-1} HEPES, pH 8.0. NFI obtained by addition of different concentrations of **Azo-2C5** ((b) 0–2.0 μmol·L^{-1}) and **Azo-2C6** ((d) 0–0.4 μmol·L^{-1}). (c,e) Hill analysis of Cl^- transport facilitated by (c) **Azo-2C5** and (e) **Azo-2C6**.

which matches the radius of K^+ (133 pm) [37], whereas the 15-crown-5 moiety has been used to construct K^+-selective channels [42] by forming a sandwich complex with K^+ [29] or construction of constitutional polarized ion channels [30]. Zeng synthesized a series of cation transporters containing 15-crown-5 or 18-crown-6 moiety as cation receptor, most of which showing high selectivity for K^+ over Na^+ [42–44]. Other crown ethers reported by Zhu [32,45], Barboiu [30,46] and Giuseppone [47] are also K^+-selective transporters. Given those literature examples of crown ether-based K^+ transporters, the inactivity of both **Azo-2C5** and **Azo-2C6** towards K^+ transport (Fig. S8) is intriguing. Valkenier, Šindelář and co-workers have reported that the transporter's extremely high affinity for NO_3^- results in the poor Cl^-/NO_3^- exchange activity [7]. Similarly in our current work, the presence of K^+ is shown to retard the Na^+ transport. We thus examined the relationship between transport activity and concentrations of K^+ (Fig. 4). We added KCl during Na^+ transport. As shown in Fig. 4(b), the addition of KCl reduced the Na^+ transport rate remarkably [29]. Similarly, addition of KCl also induced a decrease of Cl^- transport rate when **Azo-2C5** or **Azo-2C6** was used as Cl^- transporters (Fig. S10, cf. ESM). In the Cl^- transport experiment, even 1 mmol·L^{-1} of KCl can dramatically reduce the transport rate. With a NaCl or NMDG-Cl concentration of 100 mmol·L^{-1}, the addition of 1 mmol·L^{-1} KCl would exert nearly no influence on the concentration of Cl^-, and therefore the decrease of Na^+ and Cl^- transport activity can be ascribed to the presence of K^+. It is likely that because of strong K^+ affinity, the concentration of the uncomplexed transporter is low compared with that of the K^+ complex, leading to the transport process being rate-limited by the diffusion of uncomplexed transporters.

To further investigate the selectivity of the crown ether-based transporters, we performed the HPTS assay with different cations inside and outside in the presence of a pH gradient. Under the non-symmetric ionic conditions, a membrane potential would be generated if the internal and external ions have different transport rates. This would give rise to an internal pH change, the direction of which indicates the selectivity of the transporter under study [48]. With NaGlc (100 mmol·L^{-1}) outside and KGlc (100 mmol·L^{-1}) inside (Fig. S11, cf. ESM), the internal pH (indicated by the HPTS fluorescence intensity) underwent an initial decrease despite the pH outside being higher than

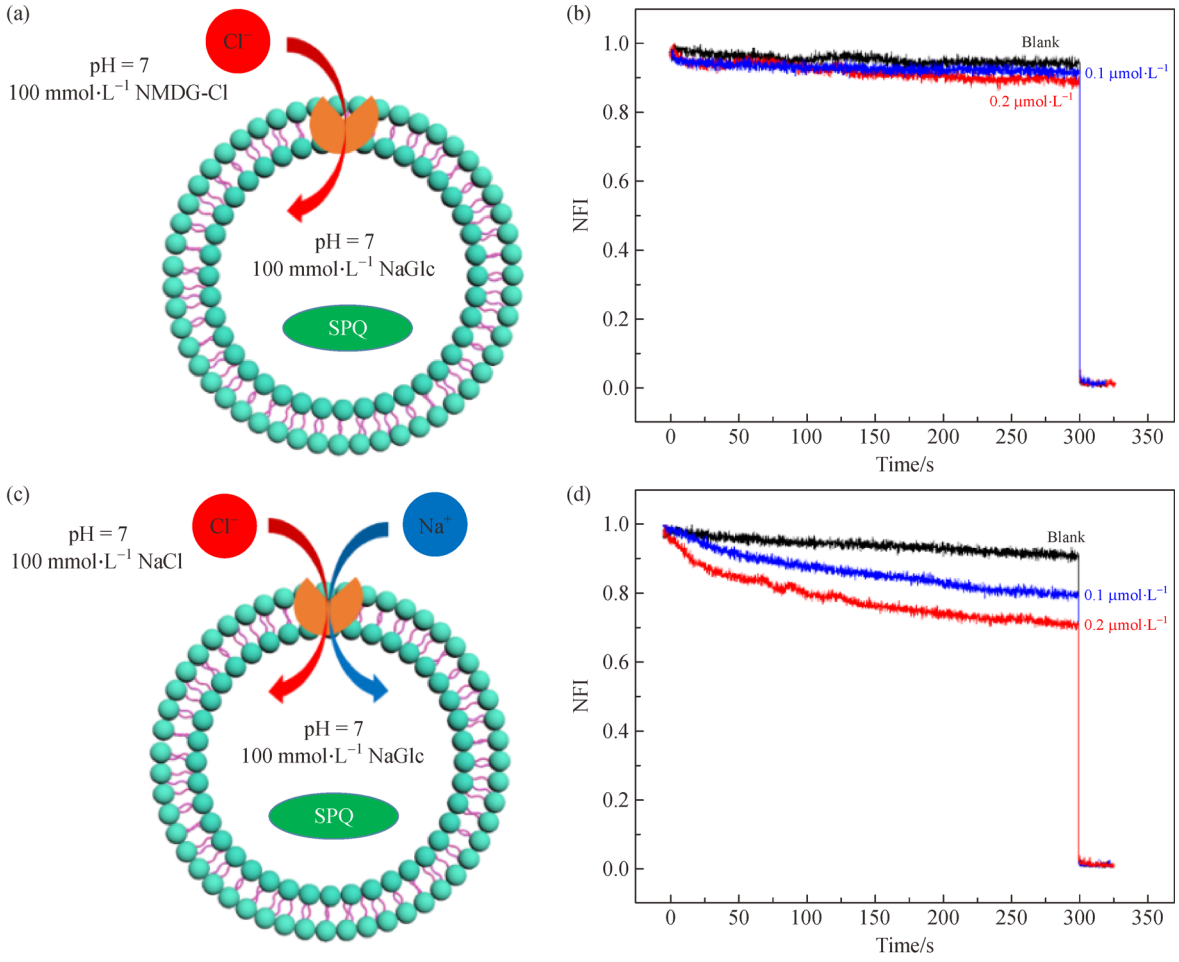

Fig. 3 (a,c) Schematic representation of SPQ experiment to verify the Cl^- transport. Inside LUVs (200 nm): 0.5 mmol·L^{-1} SPQ, 100 mmol·L^{-1} NaGlc, 10 mmol·L^{-1} HEPES, pH 7.0. Outside LUVs: (a) 100 mmol·L^{-1} NMDG-Cl or (c) NaCl, 10 mmol·L^{-1} HEPES, pH 7.0. (b,d) NFI obtained by addition of different concentrations of **Azo-2C5** (0–0.2 μmol·L^{-1}).

the pH inside, and then slowly increases following the direction of the pH gradient. The initial decrease of internal pH against the pH gradient indicates a positive membrane potential generated with K^+ outside and Na^+ inside, leading to the conclusion that the transporters are selective for K^+ over Na^+. This is consistent with the hypothesis that reduced transport activity with K^+ arises from the extremely strong K^+ binding affinity. Other transport experiments conducted when applying both a pH gradient and an ion concentration gradient (Na^+, K^+, Figs. S12 and S13, cf. ESM) also demonstrate that the transporters can transport K^+ faster than Na^+, Cl^- and H^+.

3.3 Quantitative measurement of K^+ transport

Given the diminished activity of the transporters when substantial K^+ was present outside the vesicles, we attempted to quantitatively measure the transport efficiency of K^+ by using K^+ only inside the vesicles. An HPTS assay was conducted with 100 mmol·L^{-1} of KCl inside and 100 mmol·L^{-1} NaCl outside. The driving force was a concentration gradient of K^+, since that the efflux of K^+ would generate a H^+ influx to result in the difference between starting and final pH in the vesicles (Fig. 5). At the end of the transport experiment, the final fluorescence intensity of HPTS corresponding to the transport equilibrium was obtained by the addition of Vln (10 μmol·L^{-1}) and FCCP (10 μmol·L^{-1}). The results demonstrate comparable activities of the two transporters (EC_{50} values of 0.45 μmol·L^{-1} and 0.32 μmol·L^{-1} for **Azo-2C5** and **Azo-2C6**, respectively) and also the similar Hill coefficients (n = 2.12 for **Azo-2C5**, 2.14 for **Azo-2C6**). Therefore, K^+ is assumed to be transported as a sandwich type 2:1 (transporter:K^+) complex [29,39]. The anion component was found to have negligible impact on the transport rates, as the replacement of the chloride by gluconate salt led to similar EC_{50} and n values (Fig. S14, cf. ESM, EC_{50}: 0.65 μmol·L^{-1} for **Azo-2C5**, 0.48 μmol·L^{-1} for **Azo-2C6**; n: 2.65 for **Azo-2C5**, 2.46 for **Azo-2C6**). Since K^+ has been shown to inhibit the

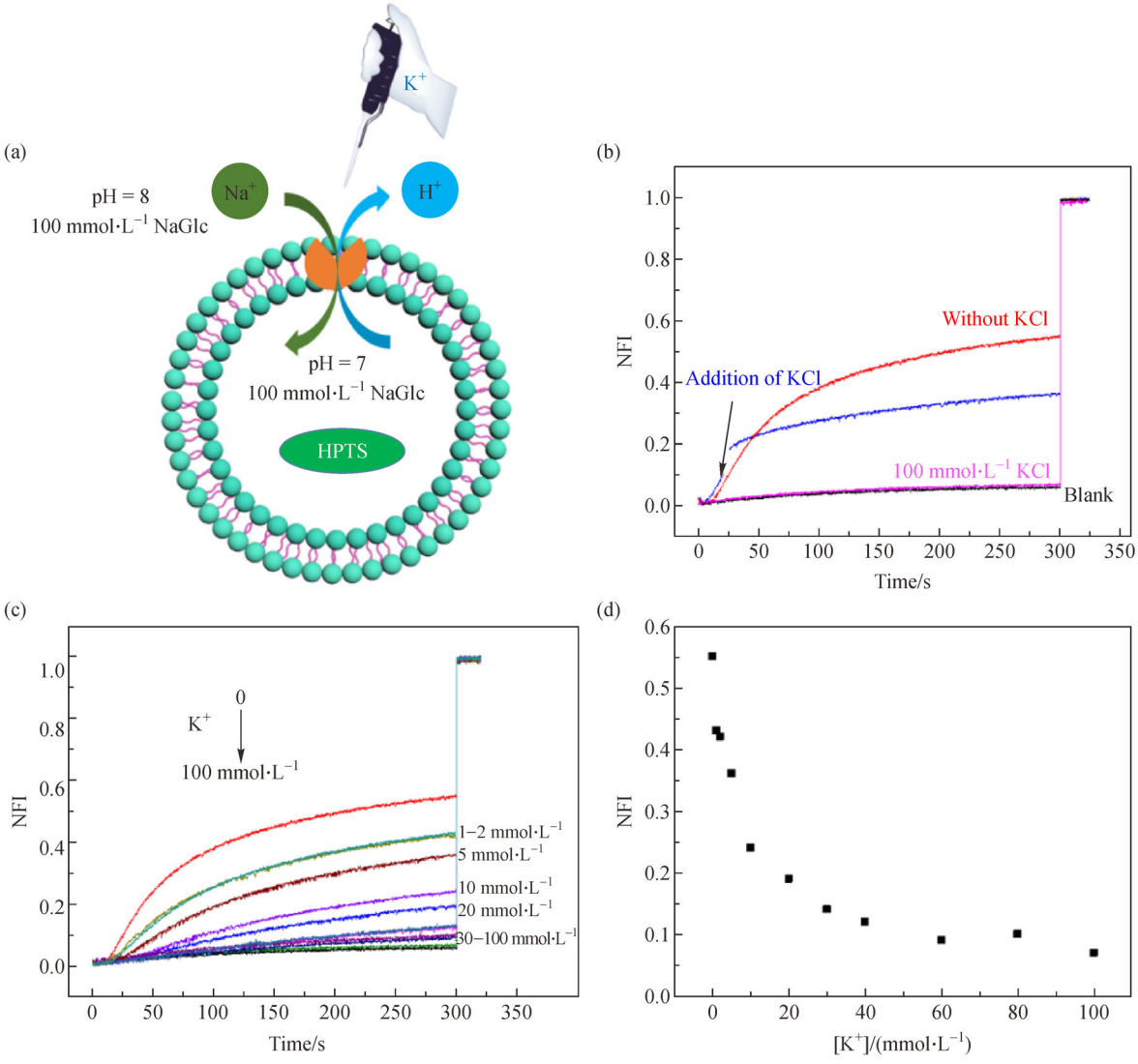

Fig. 4 (a) Schematic representation of quantitative measurement of the influence of K^+ on the Na^+ transport activity conducted by addition of different amounts of KCl to extravesicular solution before the measurement; (b) Na^+ transport activities of **Azo-2C5** (0.3 μmol·L^{-1}) measured with (red line) and without (blue line) addition of KCl (100 mmol·L^{-1}) (KCl was added after the transport process proceeded for several seconds); (c) NFI obtained by addition of **Azo-2C5** (0.3 μmol·L^{-1}) and premix of different amounts of KCl; (d) Point data of NFI measured with **Azo-2C5** (0.3 μmol·L^{-1}) and different concentrations of KCl.

transport when present at high concentrations outside vesicles (Fig. 4), by swapping the intra- and extravesicular salts (i.e., with KCl outside and NaCl inside), no transport activity was observed (Fig. S15, cf. ESM), and even when a pH gradient was applied, only a very low activity was observed (Fig. S16 , cf. ESM).

3.4 Ion transport mechanism

To better understand the unusual behavior of the transporters that depend on the identity of intervesicular and extravesicular ions, we first determined the K^+ and Na^+ binding affinities by ITC titrations. Both the compounds have higher affinities for K^+ than Na^+ in acetonitrile from ITC titration results (Figs. S17 and S18, cf. ESM, Table 1). Since significant transport activity was only observed when the external solution contains no K^+, we hypothesized that the transporters have better deliverability to the membrane when K^+ is present only inside the LUVs. To verify our assumption, the LUVs with diameters of 5 μm were prepared to measure the transporter loading capacity under different experimental conditions. The large size of the LUVs enables easy separation of the LUVs from the solution by centrifugation (Fig. S19, cf. ESM), facilitating the measurement of the transporter loading capacity by the UV-Vis absorption spectra. In the Na^+ transport experiment (Fig. 6), the transporter loading capacity (indicated by the absorption spectra of inside

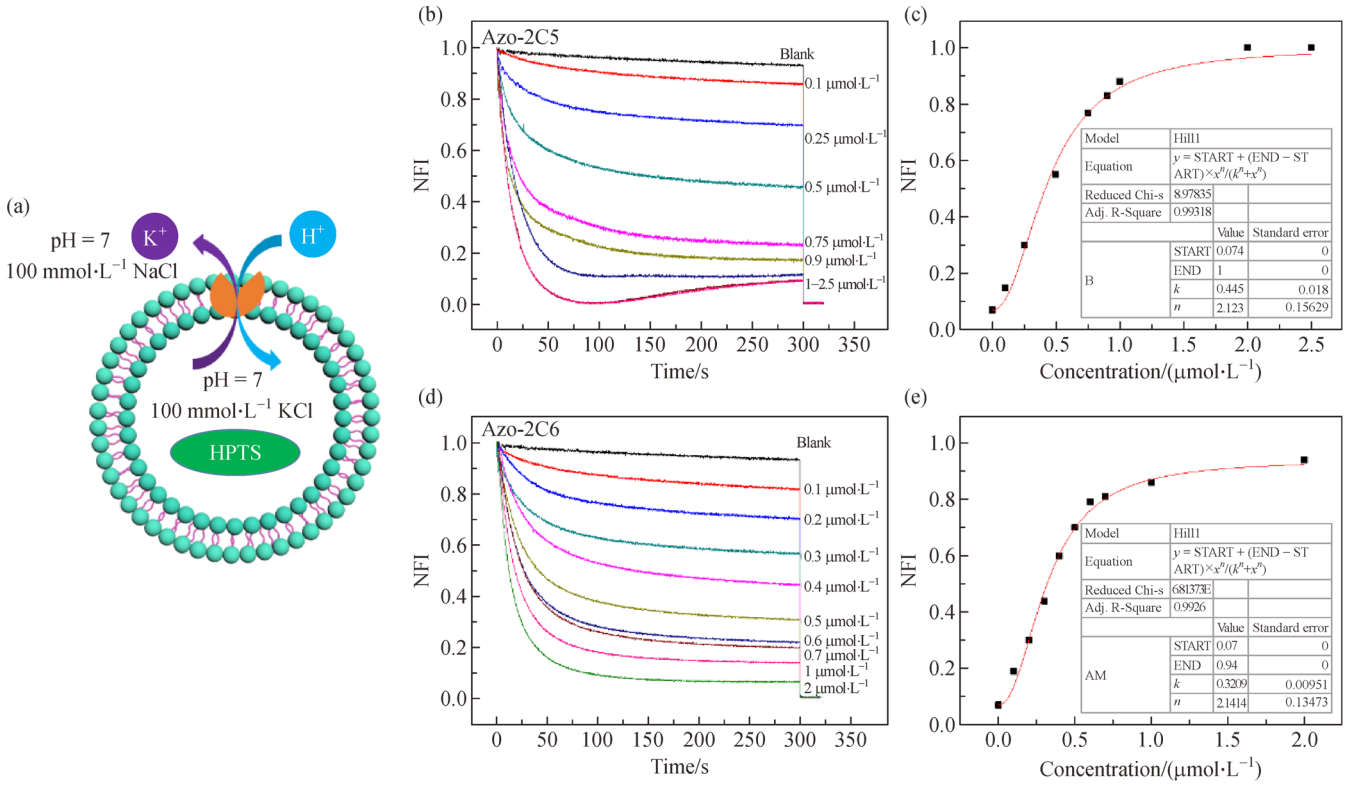

Fig. 5 (a) Schematic representation of quantitative measurement of K^+ transport (from inside to outside) conducted by exerting concentration gradient of K^+ in LUVs (mean diameter 200 nm) encapsulating pH-sensitive dye HPTS. Inside LUVs: 100 mmol·L^{-1} KCl, 10 mmol·L^{-1} HEPES, pH 7.0. Outside LUVs: 100 mmol·L^{-1} NaCl, 10 mmol·L^{-1} HEPES, pH 7.0. NFI obtained by addition of different concentrations of **Azo-2C5** ((b) 0–2.5 μmol·L^{-1}) or **Azo-C6** ((d) 0–2.5 μmol·L^{-1}). Hill analysis of K^+ uniport facilitated by (c) **Azo-2C5** or (e) **Azo-2C6**.

LUVs) decreased to a fairly low degree after the addition of K^+, which induced leaching of the transporters into the extravesicular solution. We attributed this to the strong affinity of the transporters for K^+ leading to accumulation of the transporters in the extravesicular solution when the K^+ was added, hence the low transporter loading capacity and poor transport activity. On the contrary, under the Na^+-out-K^+-in condition (Fig. S20, cf. ESM), the compounds remained in the isolated LUVs. Compared with the volume of the extravesicular solution, the intravesicular volume is much lower. Therefore, even with a high concentration of K^+ inside the vesicles, a significant portion of the transporters can partition in the membrane and facilitate ion transport. By contrast, if the extravesicular solution contains K^+, the transporters partition almost exclusively into the extravesicular solution, resulting in poor transport activity. The sum of individual absorption spectral profiles from inside and outside LUVs were comparable to the profiles of reference samples that were prepared in the same way without centrifugation, confirming the reliability of this method.

The integrity of the vesicle membrane was determined by the calcein leakage assay. Only negligible leakage of calcein occurred over 5 min (Fig. S21, cf. ESM), confirming that the crown ether-thiourea conjugates are working as transporters rather than destroying the vesicles or forming large pores [49].

Synthetic transporters can be classified as ion-channels or mobile carriers based on their working mechanism in lipid bilayers [50]. In our experiments, both the transporters seem to function as carriers for cations and anions. We prepared LUVs with DPPC, a lipid with a phase transition temperature of 41 °C, to explore the transport mechanism. Na^+ transport was completely suppressed at 31 °C, but switched on when the temperature reached 37 °C, then accelerating to a higher rate at 43 °C (Fig. 7). The transport of Cl^- and uniport of K^+ showed similar temperature-dependence in the DPPC experiments (Figs. S22 and S23, cf. ESM), indicating that both the transporters are operating as ion carriers. The DPPC experiments together with the Hill analysis data suggest that the transporters work as mobile carriers rather than ion-channels [40].

4 Conclusions

In summary, we have employed crown ether-thiourea conjugates with azobenzene linkers, i.e., **Azo-2C5** and

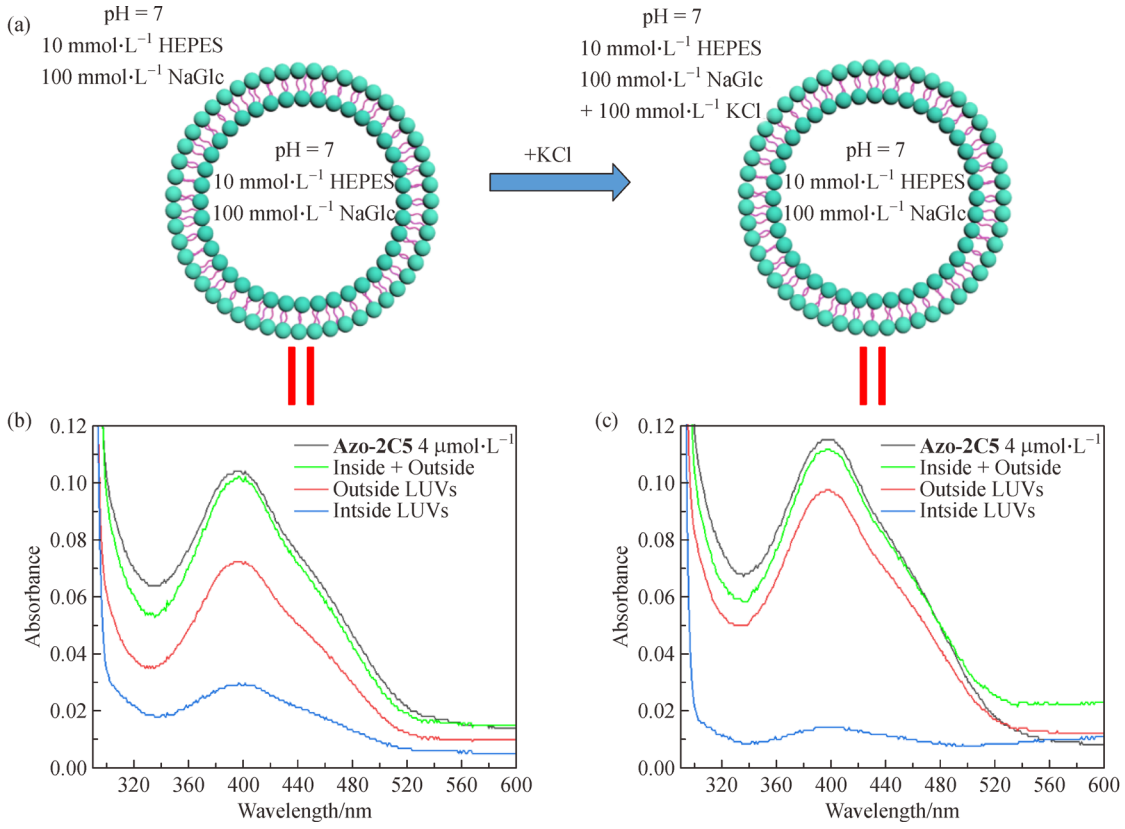

Fig. 6 (a) Schematic representation of test conditions of the absorption spectra; (b, c) Absorption spectra of **Azo-2C5** (4 μmol·L^{-1}) in lipid suspension (black line) and disperse inside (blue line, the transporters that disperse in and on the LUVs) and outside (red line, the transporters that disperse in the extravesicular solution). Absorption values of inside (blue line) and outside (red line) are added and plotted (green line) to compare with the unseparated one (black line). (b) Inside LUVs: 100 mmol·L^{-1} NaGlc, 10 mmol·L^{-1} HEPES, pH 7.0. Outside LUVs: 100 mmol·L^{-1} NaGlc, 10 mmol·L^{-1} HEPES, pH 7.0. (c) Inside LUVs: 100 mmol·L^{-1} NaGlc, 10 mmol·L^{-1} HEPES, pH 7.0. Outside LUVs: 100 mmol·L^{-1} NaGlc, 100 mmol·L^{-1} KCl, 10 mmol·L^{-1} HEPES, pH 7.0.

Table 1 Overview of the association constants and thermodynamic state functions for the 2:1 complexation of hexafluorophosphate salts with **Azo-2C5** and **Azo-2C6** as measured in acetonitrile by ITC at 30 °C

Complex	K_a/(L·mol^{-1})	n	ΔG/(kJ·mol^{-1})	ΔH/(kJ·mol$^{-1)}$	$T\Delta S$/(kJ·mol^{-1})
Azo-2C5 + Na^+	7.53 × 10^4	1.613	−28.96	−4.571	24.39
Azo-2C5 + K^+	1.82 × 10^5	2.117	−30.03	−6.101	23.93
Azo-2C6 + Na^+	4.84 × 10^4	2.043	−26.74	−1.453	25.29
Azo-2C6 + K^+	1.46 × 10^5	2.395	−29.48	−4.231	25.25

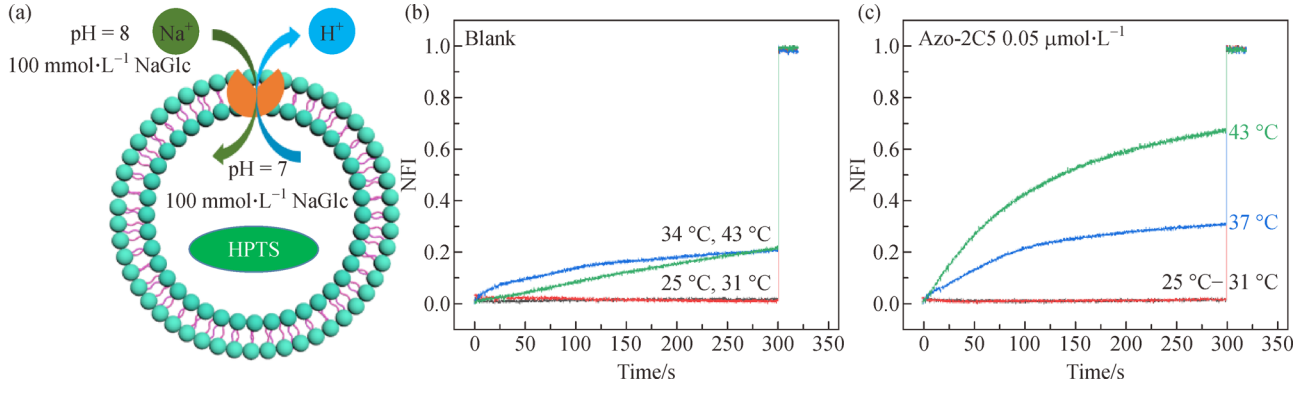

Fig. 7 (a) Schematic representation of DPPC experiments to verify the transport mechanism (ion carrier or channel). NFI obtained by addition of DMSO ((b) 20 μL) or DMSO solutions of **Azo-2C5** ((c) 0.05 μmol·L^{-1}) at different temperatures ranging from 25 °C to 43 °C.

Azo-2C6, as mobile carriers to transport the physiological important Na^+, Cl^- and K^+ ions. Though both the transporters are capable of transporting Cl^- across the membrane with considerable activity, owing to the anion binding ability of the thiourea groups, **Azo-2C5** is a much better transporter for Na^+ as its crown ether cavity (benzo-15-crown-5) fits Na^+ well. Thus **Azo-2C5** can facilitate the symport of NaCl. Moreover, the transporters' high affinity for K^+ led to predominant partitioning of the transporters in the extravesicular solution when high concentration K^+ exists outside the LUVs, leading to the suppressed ion transport activity. On the contrary, K^+ efflux facilitated by the transporters can occur when K^+ only exists inside the LUVs. These new features provide new insights into the design of cation/anion symporters and the detrimental impact of extremely strong ion binding affinity on the ion transport activity.

Acknowledgements We greatly appreciate the support of this work by the National Natural Science Foundation of China (Grant Nos. 21820102006, 91856118, 21435003 and 21521004), the MOE of China through Program for Changjiang Scholars and Innovative Research Team in University (Grant No. IRT13036), and the Scientific and Technological Plan Project in Xiamen (Grant No. 3502Z20203025).

Electronic Supplementary Material Supplementary material is available in the online version of this article at https://dx.doi.org/10.1007/s11705-021-2049-7 and is accessible for authorized users.

References

1. Wu X, Howe E N W, Gale P A. Supramolecular transmembrane anion transport: new assays and insights. Accounts of Chemical Research, 2018, 51(8): 1870–1879
2. Fyles T M. How do amphiphiles form ion-conducting channels in membranes. Lessons from linear oligoesters. Accounts of Chemical Research, 2013, 46(12): 2847–2855
3. Davis A P, Sheppard D N, Smith B D. Development of synthetic membrane transporters for anions. Chemical Society Reviews, 2007, 36(2): 348–357
4. Zhang Z, Chen J. Atomic structure of the cystic fibrosis transmembrane conductance regulator. Cell, 2016, 167(6): 1586–1597
5. Konrad M, Vollmer M, Lemmink H H, Van den Heuvel L P W J, Jeck N, Vargas-Poussou R, Lakings A, Ruf R, Deschenes G, Antignac C, et al. Mutations in the chloride channel gene CLCNKB as a cause of classic Bartter syndrome. Journal of the American Society of Nephrology, 2000, 11(8): 1449–1459
6. Dutzler R, Campbell E B, Cadene M, Chait B T, MacKinnon R. X-ray structure of a ClC chloride channel at 3.0 Å reveals the molecular basis of anion selectivity. Nature, 2002, 415(6869): 287–294
7. Valkenier H, Akrawi O, Jurček P, Sleziaková K, Lízal T, Bartik K, Šindelář V. Fluorinated bambusurils as highly effective and selective transmembrane Cl^-/HCO_3^- antiporters. Chem, 2019, 5(2): 429–444
8. Clarke H J, Howe E N W, Wu X, Sommer F, Yano M, Light M E, Kubik S, Gale P A. Transmembrane fluoride transport: direct measurement and selectivity studies. Journal of the American Chemical Society, 2016, 138(50): 16515–16522
9. Roy A, Joshi H, Ye R, Shen J, Chen F, Aksimentiev A, Zeng H. Polyhydrazide-based organic nanotubes as efficient and selective artificial iodide channels. Angewandte Chemie International Edition, 2020, 59(12): 4806–4813
10. Busschaert N, Karagiannidis L E, Wenzel M, Haynes C J E, Wells N J, Young P G, Makuc D, Plavec J, Jolliffe K A, Gale P A. Synthetic transporters for sulfate: a new method for the direct detection of lipid bilayer sulfate transport. Chemical Science (Cambridge), 2014, 5(3): 1118–1127
11. Wu X, Judd L W, Howe E N W, Withecombe A M, Soto-Cerrato V, Li H, Busschaert N, Valkenier H, Perez-Tomas R, Sheppard D N, et al. Nonprotonophoric electrogenic Cl^- transport mediated by valinomycin-like carriers. Chem, 2016, 1(1): 127–146
12. Davis J T, Gale P A, Quesada R. Advances in anion transport and supramolecular medicinal chemistry. Chemical Society Reviews, 2020, 49(16): 6056–6086
13. Ren C, Zeng F, Shen J, Chen F, Roy A, Zhou S, Ren H, Zeng H. Pore-forming monopeptides as exceptionally active anion channels. Journal of the American Chemical Society, 2018, 140(28): 8817–8826
14. Spooner M J, Li H, Marques I, Costa P M R, Wu X, Howe E N W, Busschaert N, Moore S J, Light M E, Sheppard D N, et al. Fluorinated synthetic anion carriers: experimental and computational insights into transmembrane chloride transport. Chemical Science (Cambridge), 2019, 10(7): 1976–1985
15. Gokel G W, Mukhopadhyay A. Synthetic models of cation-conducting channels. Chemical Society Reviews, 2001, 30(5): 274–286
16. Yu F H, Catterall W A. Overview of the voltage-gated sodium channel family. Genome Biology, 2003, 4(3): 207
17. Goldin A L. Resurgence of sodium channel research. Annual Review of Physiology, 2001, 63(1): 871–894
18. Payandeh J, Scheuer T, Zheng N, Catterall W A. The crystal structure of a voltage-gated sodium channel. Nature, 2011, 475 (7356): 353–358
19. Ryan D P, Ptacek L J. Episodic neurological channelopathies. Neuron, 2010, 68(2): 282–292
20. Jentsch T J. Neuronal KCNQ potassium channels: physiology and role in disease. Nature Reviews. Neuroscience, 2000, 1(1): 21–30
21. Sanguinetti M C, Tristani-Firouzi M. hERG potassium channels and cardiac arrhythmia. Nature, 2006, 440(7083): 463–469
22. Russell J M. Sodium-potassium-chloride cotransport. Physiological Reviews, 2000, 80(1): 211–276
23. Simon D B, Karet F E, Hamdan J M, Pietro A D, Sanjad S A, Lifton R P. Bartter's syndrome, hypokalaemic alkalosis with hypercalciuria, is caused by mutations in the Na-K-2Cl cotransporter NKCC2. Nature Genetics, 1996, 13(2): 183–188
24. Tong C C, Quesada R, Sessler J L, Gale P A. Meso-Octamethylcalix [4]pyrrole: an old yet new transmembrane ion-pair transporter. Chemical Communications, 2008, (47): 6321–6323
25. Fisher M G, Gale P A, Hiscock J R, Hursthouse M B, Light M E, Schmidtchen F P, Tong C C. 1,2,3-Triazole-strapped calix[4] pyrrole: a new membrane transporter for chloride. Chemical

Communications, 2009, 21(21): 3017–3019
26. Koulov A V, Mahoney J M, Smith B D. Facilitated transport of sodium or potassium chloride across vesicle membranes using a ditopic salt-binding macrobicycle. Organic & Biomolecular Chemistry, 2003, 1(1): 27–29
27. Lee J H, Lee J H, Choi Y R, Kang P, Choi M G, Jeong K S. Synthetic K^+/Cl^--selective symporter across a phospholipid membrane. Journal of Organic Chemistry, 2014, 79(14): 6403–6409
28. Yu X H, Cai X J, Hong X Q, Tam K Y, Zhang K, Chen W H. Synthesis and biological evaluation of aza-crown ether-squaramide conjugates as anion/cation symporters. Future Medicinal Chemistry, 2019, 11(10): 1091–1106
29. Sun Z, Barboiu M, Legrand Y M, Petit E, Rotaru A. Highly selective artificial cholesteryl crown ether K^+-channels. Angewandte Chemie International Edition, 2015, 54(48): 14473–14477
30. Gilles A, Barboiu M. Highly selective artificial K^+ channels: an example of selectivity-induced transmembrane potential. Journal of the American Chemical Society, 2016, 138(1): 426–432
31. Li Y H, Zheng S, Legrand Y M, Gilles A, van der Lee A, Barboiu M. Structure-driven selection of adaptive transmembrane Na^+ carriers or K^+ channels. Angewandte Chemie International Edition, 2018, 57(33): 10520–10524
32. Chen S, Wang Y, Nie T, Bao C, Wang C, Xu T, Lin Q, Qu D H, Gong X, Yang Y, Zhu L, Tian H. An artificial molecular shuttle operates in lipid bilayers for ion transport. Journal of the American Chemical Society, 2018, 140(51): 17992–17998
33. Wu F Y, Li Z, Guo L, Wang X, Lin M H, Zhao Y F, Jiang Y B. A unique NH-spacer for *N*-benzamidothiourea based anion sensors. Substituent effect on anion sensing of the ICT dual fluorescent *N*-(p-dimethylaminobenzamido)-*N′*-arylthioureas. Organic & Biomolecular Chemistry, 2006, 4(4): 624–630
34. Li A F, Wang J H, Wang F, Jiang Y B. Anion complexation and sensing using modified urea and thiourea-based receptors. Chemical Society Reviews, 2010, 39(10): 3729–3745
35. Villa M, Bergamini G, Ceroni P, Baroncini M. Photocontrolled self-assembly of azobenzene nanocontainers in water: light-triggered uptake and release of lipophilic molecules. Chemical Communications, 2019, 55(79): 11860–11863
36. Du Z, Ren B, Chang X, Dong R, Peng J, Tong Z. Aggregation and rheology of an azobenzene-functionalized hydrophobically modified ethoxylated urethane in aqueous solution. Macromolecules, 2016, 49(13): 4978–4988
37. Otis F, Racine-Berthiaume C, Voyer N. How far can a sodium ion travel within a lipid bilayer? Journal of the American Chemical Society, 2011, 133(17): 6481–6483
38. Yang Y, Wu X, Busschaert N, Furuta H, Gale P A. Dissecting the chloride-nitrate anion transport assay. Chemical Communications, 2017, 53(66): 9230–9233
39. Vargas Jentzsch A, Emery D, Mareda J, Metrangolo P, Resnati G, Matile S. Ditopic ion transport systems: anion-π interactions and halogen bonds at work. Angewandte Chemie International Edition, 2011, 50(49): 11675–11678
40. Busschaert N, Wenzel M, Light M E, Iglesias-Hernandez P, Perez-Tomas R, Gale P A. Structure-activity relationships in tripodal transmembrane anion transporters: the effect of fluorination. Journal of the American Chemical Society, 2011, 133(35): 14136–14148
41. Valkenier H, Haynes C J E, Herniman J, Gale P A, Davis A P. Lipophilic balance—a new design principle for transmembrane anion carriers. Chemical Science (Cambridge), 2014, 5(3): 1128–1134
42. Ren C, Shen J, Zeng H. Combinatorial evolution of fast-conducting highly selective K^+-channels via modularly tunable directional assembly of crown ethers. Journal of the American Chemical Society, 2017, 139(36): 12338–12341
43. Ren C, Chen F, Ye R, Ong Y S, Lu H, Lee S S, Ying J Y, Zeng H. Molecular swings as highly active ion transporters. Angewandte Chemie International Edition, 2019, 58(24): 8034–8038
44. Ye R, Ren C, Shen J, Li N, Chen F, Roy A, Zeng H. Molecular ion fishers as highly active and exceptionally selective K^+ transporters. Journal of the American Chemical Society, 2019, 141(25): 9788–9792
45. Liu T, Bao C, Wang H, Lin Y, Jia H, Zhu L. Light-controlled ion channels formed by amphiphilic small molecules regulate ion conduction via cis-trans photoisomerization. Chemical Communications, 2013, 49(87): 10311–10313
46. Sun Z, Gilles A, Kocsis I, Legrand Y M, Petit E, Barboiu M. Squalyl crown ether self-assembled conjugates: an example of highly selective artificial K^+ channels. Chemistry (Weinheim an der Bergstrasse, Germany), 2016, 22(6): 2158–2164
47. Schneider S, Licsandru E D, Kocsis I, Gilles A, Dumitru F, Moulin E, Tan J, Lehn J M, Giuseppone N, Barboiu M. Columnar self-assemblies of triarylamines as scaffolds for artificial biomimetic channels for ion and for water transport. Journal of the American Chemical Society, 2017, 139(10): 3721–3727
48. Wu X, Small J R, Cataldo A, Withecombe A M, Turner P, Gale P A. Voltage-switchable HCl transport enabled by lipid headgroup-transporter interactions. Angewandte Chemie International Edition, 2019, 58(42): 15142–15147
49. Wu X, Busschaert N, Wells N J, Jiang Y B, Gale P A. Dynamic covalent transport of amino acids across lipid bilayers. Journal of the American Chemical Society, 2015, 137(4): 1476–1484
50. Zheng S P, Huang L B, Sun Z, Barboiu M. Self-assembled artificial ion-channels toward natural selection of functions. Angewandte Chemie International Edition, 2021, 60(2): 566–597